Functional Cotton Fiber-Based TLC-SERS Matrix for Rapid and Sensitive Detection of Mixed Dyes

Huifang Yao
Hubei University of Police
Xiaxiao Dong
Hubei University
Hong Xiong
Hubei University
Ji Zhou (zhouji@hubu.edu.cn)
Hubei University https://orcid.org/0000-0003-4688-4983
Yong Ye
Hubei University

Research Article

Keywords: organic dye, thin layer chromatography (TLC), surface enhanced Raman spectroscopy (SERS), β-Cyclodextrin, cotton fabric

Posted Date: March 3rd, 2022

DOI: https://doi.org/10.21203/rs.3.rs-1311714/v1

Abstract

A facile cotton fabric with a built-in TLC-SERS structure was fabricated to demonstrate an integrated TLC separation and SERS identification of mixed dyes. The soft and flexible SERS fabric was firstly fabricated using a simple method in which gold nanoparticles were *in-situ* synthesized on cotton fabrics by heating. β-CD was then grafted onto cotton fabric through crosslinking with citric acid in presence of sodium hypophosphite monohydrate via esterification reaction. The adsorption and TLC development performance of β-CD grafted fabrics were comprehensively investigated with two representative organic dyes, one anionic dye and one nonionic dye. Besides, the recyclable adsorption and separation performance were tested to evaluate its sustainable application prospects. It displayed less adsorption capacity loss and reusable separation performance after several cycles than the pristine cotton fabrics. Finally, two sets of mixed dyes were successfully separated on the TLC fabrics and then identified *via* on-site SERS according to their different migration distance. The developed TLC-SERS fabric shows the advantage of quick, easy to handle, low-cost, sensitive, and could be exploited in *on-site* study of synthetic dyes in art objects, textile and packaging products or forensic applications.

Introduction

Organic dyes, embedding into various matrices (such as: textiles, coating, plastic, or food additives and packaging) with low concentrations, are broadly used for the excellent color performance which satisfies people's color consumption needs. The *on-site* identification of dyestuffs, especially in forensic studies, cultural heritage, dating and authentication research of artworks as well as quality controls of products (textile, lipstick, cosmetic, or food packaging), is challenging due to numbers of complexities and small amounts of samples (Boscacci et al. 2020; Cañamares et al. 2014; Cesaratto et al. 2019; Kong et al. 2017; Pozzi et al. 2013; Woodhead et al. 2016).

Due to its extreme sensitivity, fingerprint-based high specificity and capacity in simultaneous detection of multi-analytes, surface enhanced Raman spectroscopy (SERS) is a powerful tool for dyestuff identification on limited amount of samples as well as by means of *on-site* set ups (Pilot 2018). Although SERS technology has developed rapidly in recent years, it does not always allow for reliable differentiation of several components in a mixture due to the interference effect of matrix. To overcome these limits, necessary pretreatment and separation technology such as solid phase microextraction (SPME), thin layer chromatography (TLC), gas chromatography (GC), and liquid chromatography (LC) are needed to operate before the quantitative or semi-quantitative identification.

Compared with the separation techniques such as GC and LC, TLC is undoubtedly a powerful technique since the separation can be done *on-site* rapidly without the requirement of high-cost instruments or skilled persons (Zhang et al. 2014). Moreover, it also shows unique advantages such as low cost, less sample pretreatment, low usage of solvents and high throughput of TLC screening on a single plate. Recently, thin layer chromatography coupled with surface enhanced Raman spectroscopy (TLC-SERS), showing great performance of preliminary TLC screening along with on-site SERS identification, has been

quickly developed and widely applied to separate and detect complex ingredients (Fang et al. 2016; Freye et al. 2013; Li et al. 2011; Sciutto et al. 2017; Weatherston et al. 2019). Usually, the routine TIC-SERS analysis requires isolation of the mixture on a TLC plate following a common TLC procedure. Afterwards, metallic nanoparticles were dropped on the separated spots or spayed on the whole TLC plate, and then the SERS spectra were collected from the separated spot to identify the information of the surface components. Researches of TLC-SERS were conducted on the analysis of medicinal herbs (Gu et al. 2018; Li et al. 2021; Minh et al. 2019; Rojanarata et al. 2013), dyes (Cañamares et al. 2014; Pereira et al. 2018; Pozzi et al. 2013), environmental pollutants (Li et al. 2011; Shen et al. 2021b), food prohibited additives (Kong et al. 2017; Qu et al. 2018; Shen et al. 2021a; Soares et al. 2017), dietary supplements (Li et al. 2015) and so on. It is worth mentioning that TLC coupled with SERS mapping could be exploited in *on-site* monitoring the processes of chemical reactions (Zhang et al. 2014). So far, various means, such as types of the TLC plates (silica gel, cellulose or diatomite), and various chemometric tools for data analysis (support vector machine (Tan et al. 2019) or quaternion principal component analysis (Zhao et al. 2019)) were conducted to realize wider practical applications. Despite these enormous progresses, the post-modification of metallic nanoparticles may bring some troubles for SERS analysis. Whether the nanoparticles are hydrophilic or hydrophobic, both the nanoparticles and analytes would be redistributed on the TLC plate. The “coffee-ring effect” would also generate the migration of nanoparticles and analytes, resulting in the efficacy and repeatability of SERS performance (Minh et al. 2019; Zhu et al. 2019; Zhu et al. 2016). It is noticed that usage of porous materials such as metal – organic frameworks (MOFs) (Schenk et al. 2017; Zhang et al. 2018) or electrospun polymeric nanofibers (Rojanarata et al. 2013) in TLC can offer new input and be endowed with multi-function towards various applications. Therefore, it would be in demand to attempt preparation of a porous TLC plate with a built-in SERS structure for an integrated TLC-SERS detection.

Cotton fabric is inexpensive, biocompatible, biodegradable, portability, and allows a sample fluid to flow by capillary force. Various methods have been developed for chemical modification of cotton fabrics for sample pretreatment, such as sample storage and collection, sample separation, and sample preconcentration (Tang et al. 2019). Cotton fibers have also been reported to act as reducing agents to *in situ* synthesize Au NPs or Ag NPs, which can act as flexible SERS substrates for analysis of dyes on fabrics (Tang et al. 2017). Therefore, cotton fabric is a facile alternative material for TLC separation including the integrated use for *in situ* SERS analysis. Though cotton fabrics with their inherent ability of capillary-action fluidic could be used for sample separation, it is necessary to explore a stable and efficient media on pristine cotton fabrics. β-cyclodextrin (β-CD), the most common and commercially available type of cyclodextrins with a macrocycle of seven glucose units, has an external surface which is hydrophilic and an inner cavity that is hydrophobic. The porous β-CD stationary phase has high separation efficiency, good resolution, stable physical and chemical properties, and low price (Xiao et al. 2012). Various separation application are explored *via* cross-linking of β-CD with silica (Bao et al. 2021), COFs (Wang et al. 2021) or graphene (Wu et al. 2019) as stationary phase. Cotton fibers, a natural cellulose polymer, with the chemical similarity of glucose units to β-CD could be considered as a potential β-CD carrier. Moreover, the fabric significantly outperforms, in terms of its good dimensional stability,

sustainable application prospects and the development of value-added multifunctional textiles (Alzate-Sánchez et al. 2016; Ma et al. 2020).

Herein, the objective of this research is to explore a facile TLC fabric with a built-in SERS structure for an integrated TLC-SERS detection. To accomplish the preliminary TLC screening along with on-site SERS identification, the SERS fabric was fabricated using a simple method in which gold nanoparticles were *in-situ* synthesized on cotton fabrics by heating. Porous β-CD was then covalently grafted onto cotton fabric via esterification reaction. The characterization, adsorption property, TLC development performance and sustainable application were conducted. Furthermore, two sets of mixed dyes were separated on the TLC fabrics and then identified via SERS according to the migration distance, which showed that the developed TLC-SERS fabric could be exploited in *on-site* study of synthetic dyes in art objects, textile and packaging products or forensic applications.

Experimental Section

Materials

β-cyclodextrin (β-CD, ≥ 98%) and potassium phosphate monobasic (KH_2PO_4, ≥ 99.5%) were purchased from Aladdin (Shanghai, China). Citric acid monohydrate ($C_6H_8O_7{\cdot}H_2O$, CA, ≥ 99.5%), sodium hypophosphite monohydrate ($NaH_2PO_2{\cdot}H_2O$, SHP, ≥ 99.5%), tetrachloroauric (III) acid trihydrate ($HAuCl_4{\cdot}3H_2O$, > 99%), ammonia solution, hydrochloric acid, ethanol (≥ 99.7%), methanol, dichloromethane, ethyl acetate, cyclohexane, n-Butanol were purchased from Sinopharm Chemical Reagent (Shanghai, China). Rhodamine B (RhB), sudan Ⅲ (SD), malachite green (MG), congo red (CR) were obtained from Macklin (Shanghai, China). All chemicals were analytic grade reagents, and used without further purification. Knitted cotton fabrics were obtained from a local retailer. Deionized water from a Milli-Q Millipore system was used for all the experiments.

Instruments

Morphology of the cotton fabrics were performed using a scanning electron microscope (SEM) (FEI Quanta 200). X-ray diffraction (XRD) patterns were recorded using a Bruker D8 Advance X-ray diffractometer with Cu Kα radiation (2θ = 5°-70°). UV-vis absorption spectra were obtained with an Ocean Optics USB4000 Spectrometer and recorded using Ocean Optics SpectraSuite software. Cary 600 series Fourier-transformed infrared (FTIR) spectrometer (Agilent Technologies) equipped with an attenuated total reflection (ATR) attachment was used to measure the FTIR spectra. Hydrophilic properties were evaluated by contact angle measurement using an OCA 40 Micro optical contact angle system (Dataphysics). 5 μL of water droplets were deposited directly on the surface of the fabrics and the water contact angles (WCAs) were measured. SERS analysis was performed under the 785 nm excitation line of a high power diode laser (> 280 mW) on an inVia Reflex confocal micro-Raman spectrometer (Renishaw, UK). The SERS signal was collected over the wavenumber range of 200–1800 cm^{-1} with an integration time of 10 s and 0.5% of the laser power by a single scan.

Preparation of Cot@β-CD

The modification of cotton fabrics with β-CD was based on the protocol reported previously (Patil and Netravali 2019), as illustrated in Scheme 1. 0.50 g KH_2PO_4, 1.09 g $C_6H_8O_7{\cdot}H_2O$ and 2.00 g β-CD were sequentially added into 45.0 mL deionized water under constant stirring for 5 min. The obtained mixture was hydrothermally reacted at 140 ℃ for 180 min. The color of the solution changed from colorless to light yellow. 4.0 g SHP was then added to the yellow solution with stirring and then kept at room temperature. Knitted cotton fabrics (denoted as Pri-Cot, 1.0 cm × 7.5 cm) were shaken and washed for 3 min with warm water (50 ℃) followed by rinsing with deionized water at room temperature. The washed fabrics were immersed in the prepared mixed aqueous solutions for 5 min, then they were placed between two glass plates and squeezed twice. After squeezing out the excess solution, the pressed fabrics were transferred into oven and heated at 180 ℃ for 10 min. Then the β-CD modified fabrics (denoted by Cot@β-CD) were rinsed with running deionized water and dried at room temperature. The cross linking of β-CD to the cotton fabric via esterification with the polycarboxylic acid was generated during the pad-dry-cure process. The grafting percentage of the treated fabrics can use the following equation:

$$graftingpercentage = \frac{W_t - W_c}{W_c} \times 100$$

where W_t is the weight of the treated fabrics after modification with β-CD and W_c is the weight of the knitted cotton fabrics (Patil and Netravali 2019).

Preparation of Cot@Au NPs@β-CD

According to our previous reports (Tang et al. 2017), the SERS-active cotton fabrics were fabricated as follows: the washed fabrics were incubated in $HAuCl_4$ aqueous solutions (0.125 mM) for 10 min. The weight ratio of aqueous solution to fabrics was 100:1. The solutions were then heated at 85 ℃ for 90 min in a shaking water bath. The Au NPs modified fabrics (denoted by Cot@Au NPs) were then rinsed with running deionized water and dried at room temperature. The next β-CD modified step was the same as procedure 2.3 described. The Cot@Au NPs were immersed into the mixed solution and then hot-pressed to graft with β-CD. The obtained fabrics were designated as Cot@Au NPs@β-CD.

Adsorption performance of organic dyes with Cot@β-CD

In order to investigate the dye adsorption performance of the treated cotton fabric, four dyes (MG, RhB, CR and SD) were selected. ~ 12.5 mg of cotton fabrics (Pri-Cot, Cot@β-CD, Cot@Au NPs and Cot@Au NPs@β-CD) were added into 1 mL of 1×10^{-4} M of different organic dyes solutions under constant stirring. UV-vis absorption spectra of the dye solution with or without the fabrics were collected.

MG was selected as a target dye to investigate the regeneration ability of β-CD modified fabric. Pri-Cot and Cot@β-CD pieces (0.8 cm×0.8 cm) were incubated with 1.0 mL dye solution for 24 h to establish the adsorption/desorption equilibrium. Then the fabrics were taken out and the residual MG solutions were

detected on a UV–vis spectrophotometer. The removal efficiency (η) of the cotton fabrics were calculated as follows:

$$\eta = \frac{C_0 - C}{C_0} \times 100\%$$

where, C_0 and C are the initial and final concentration of dye in the aqueous phase, respectively. A mixture of ethanol and 0.5 M HCl (v/v = 4:3) was employed to realize desorption of MG. The Pri-Cot and Cot@β-CD pieces were immersed in the above solvents for 180 min at room temperature and then rinsed in deionized water, followed by drying at room temperature. And the removal efficiency (η) of each cycle was compared.

TLC separation and SERS identification

TLC separation

Two sets of sample solutions (MG/SD and RhB/SD) were obtained by mixing the relevant dye solutions with the volume ratio of 1:1. The Cot@β-CD and Cot@Au NPs@β-CD fabrics were evenly stuck on the surface of the glass slide. Dyes solutions and mixtures were spotted onto the position at 10 mm from the bottom of the treated fabrics by using a capillary with a diameter of 0.6 mm. The solutions were spotted three times. TLC fabrics were then placed into the glass chamber containing 2 mL of mobile phase. After equilibrating for 5–10 min, TLC separation was performed using a mixture of dichloromethane: methanol (3:1, v/v) as optimized mobile phase solvent. All the TLC fabrics were developed until the mobile phase reached at least a migration distance of 60 mm. After the solvent on the TLC fabrics evaporated naturally, the separated sample spots were visualized by the absorbance or fluorescence. Digital photographs were obtained for each separation using a digital camera. The retention factor (R_f) value is defined as the distance travelled by the separated sample divided by the distance travelled by the solvent. Every fabric was developed three times and the R_f values of separated samples were recorded.

Recyclable TLC separation performance

The regeneration of the TLC separation was conducted to verify its sustainable application. The mixed and separated dye solution were eluted with solvent of ethanol and 0.5 M HCl (v/v = 4:3), and the next TLC separation step was conducted as describes in TLC separation procedure above.

SERS identification

The TLC-SERS method (shown in Scheme. 1) was designed for on-site detection of MG/SD and RhB/SD. First, 0.5 mL of mixed sample was spotted on the bottom of a TLC plate and chromatography was performed in a developing chamber with 3/1 (v/v) dichloromethane/methanol as the optimal mobile phase. The separated spots were visualized by their own color or according to their different R_f values. Finally, a SERS spectrum for each separated spot was recorded using a Raman spectrometer with the 785

nm excitation line, allowing qualitative analysis of the components of the analyte mixture. All the measurements were repeated in triplicate.

Results And Discussion

Morphology and structure of the treated cotton fabrics

Structures of the functionalized cotton fabrics before and after grafting were investigated by comparative inspection of their XRD curves and FTIR spectra. The XRD curves of the four treated fabrics are shown in Fig. 1a. In the XRD pattern of Pri-Cot, the characteristic peaks of cellulose I at 14.8°, 16.8° and 22.8° were found (French and Cintrón 2013). Another moderate peak appeared near 34.3° has Miller index (004) and is not the dominant contributor of the intensity (French 2014). The additional weak peaks at a 2θ value of 38.5° in the XRD pattern of Cot@Au NPs and Cot@Au NPs@β-CD fabric are assigned to the (111) crystal planes of gold (Kim et al. 2006), revealing that Au NPs were formed on fabrics via *in situ* reduction. In addition, the diffraction patterns of cellulose I in these fabrics are not altered greatly. Due to that the cyclodextrin molecules are bonded to the surfaces of the cryrstallites, probably in a random manner, and that the molecules within the crsytallite interiors are not derivatized. The crystallite size of cellulose I can be calculate by Scherrer equation $\tau = K\lambda / \beta\cos\theta$, τ (Å) is the size perpendicular to the lattice plane represented by the peak in question, K is a constant that depends on the crystal shape, λ is the wavelength of the incident beam in the diffraction experiment, β is the full width at half maximum (FWHM) of the refelction peak in radians and θ is the position of the peak (half of the plotted 2-θ value) (French and Cintrón 2013). After cotton fabrics were modified by Au NPs and β-CD, the crystallite sizes of cellulose I in fabrics were almost the same (60 Å), further indicating that the modification did not affect the crystal structure which agreed with the not high grafting percentage (6.75%). Chemical structure and interactions between β-CD and cotton fabric were analyzed by FTIR spectroscopy. As shown in Fig. 1b, three spectral regions presented in the case of Pri-Cot: a broad band occurred at 3200–3500 cm^{-1}, which is assigned to O – H stretching; two peaks at 2919 and 2852 cm^{-1} are attributed to the asymmetric and the symmetric stretching of methylene (-CH_2-) groups in the long alkyl chains; the bands in the range of 1500 – 800 cm^{-1} appeared as a result of C-H, O-H, C-O, and C-O-C vibrations, representing the fingerprint of cellulose (Tang et al. 2012). After grafting with β-CD, a new band was appeared at 1720 cm^{-1} compared with the Pri-Cot and Cot@Au NPs, which should be attributed to the carbonyl groups from the ester bonds (Patil and Netravali 2019). This result confirmed that β-CD was successfully grafted onto cotton fiber through polyesterification reaction. The hydroxyl groups of cellulose and those of β-CD react with the polycarboxylic acid to give esters.

SEM was employed to observe the surface morphologies of the treated cotton fabrics. Figure 2a show the SEM image of the Pri-Cot fabric. Grooves and fibrils were clearly observed on the surface of the fabric. The Cot@β-CD shows a rougher surface appearance. A number of flakes were also found over the surface of fibers (Fig. 2b). The polymer β-CD was observed to form bridges between neighboring cotton yarns. Figure 2c shows the SEM image of Cot@Au NPs, a number of nanoparticles were seen over the

surface of fibers, demonstrating that Au NPs were *in situ* synthesized on cotton. Number of flakes and nanoparticles could be clearly found on the surface of the Cot@Au NPs@β-CD fabrics (Fig. 2d). The color of cotton fabrics treated with Au NPs were deep-purple (inset photograph of Fig. 2c and d), which also implies the presence of Au NPs on cotton fibers.

Hydrophilic surface properties of the treated cotton fabrics before and after grafting with β-CD and Au NPs were tested. In the water contact angle test, as shown in Fig. 3, the four fabrics exhibit superhydrophilicity in air with contact angles of nearly 0°. The water drop penetrated into the Pri-Cot, Cot@β-CD and Cot@Au NPs@β-CD within 30 ms, while penetrating into the Cot@Au NPs within 1 s. It is obviously noted that functionalization of cotton fabrics by β-CD improves significantly the hydrophilicity because of the abundant surface hydroxyl groups. The modification of Au NPs may increase the surface roughness, resulting the slightly longer contact time of the water drop and the fabric.

Adsorption performance of the treated fabrics toward organic dyes

Four representative organic dyes (positively charged malachite green (MG^+), positively charged rhodamine B (RhB^+), negatively charged congo red (CR^-), and neutrally charged sudan Ⅲ (SD^0)) with different charges were used as probes to evaluate the affinity between dyes and the treated fabrics *via* UV–vis adsorption spectroscopy in this work. Figure 4a-d showed the UV–vis adsorption spectra obtained from the organic dye solution or residual dye solution after it was incubated with Pri-Cot, Cot@β-CD, Cot@Au NPs and Cot@Au NPs@β-CD fabric for 24 h. The dye solutions show strong absorption peaks at 617 nm, 559 nm, 496 nm and 506 nm, for MG^+, RhB^+, CR^- and SD^0, respectively. If the fabrics could absorb more dyes, few dyes would be residual in solution, and thus lower absorption intensity will be observed. From Fig. 4a and b, it is observed, the absorption peak intensity for MG^+ and RhB^+ sharply dropped after dye solution was incubated with Cot@β-CD and Cot@Au NPs@β-CD fabric, while decreased slowly with Pri-Cot and Cot@Au NPs. Besides, the adsorption for MG^+ and RhB^+ on Pri-Cot and Cot@Au NPs showed different results, which may be related to the different affinity between cationic dyes and Au NPs. Compare with MG^+ and RhB^+, opposite results were observed for CR^- (Fig. 4c). The absorption peak intensity of residual dye solution decreased slightly after incubating with Cot@β-CD and Cot@Au NPs@β-CD fabric, while dropped sharply with Pri-Cot and gradually for Cot@Au NPs. For SD^0, all the four fabrics showed no significant absorption ability. These results shown in Fig. 4a-d indicated that the presence of β-CD provides the enhanced adsorption ability to fix the cationic dye molecules. Interactions between β-CD treated fabrics and cationic dye molecules are due to the following: (i) complexation of dye molecules using β-CD host molecules and (ii) plenty of dehydrogenated carboxylic acid of citric acid, resulting in a strong negative charge on the modified cotton fabric. The electrostatic and the host-guest interaction boosted the adsorption of cationic dyes MG and RhB on β-CD finishing cotton fabrics.

Generally, the stability and recyclable adsorption of the finishing fabrics is one of the most significant factors for sustainable applications. It was reported that upon curing the treated cotton fabric at 180°C,

ester linkage were formed between CA and both cellulose and β-CD (Abdel-Halim et al. 2014). Therefore, the β-CD moieties have the potential capability of realizing recyclable adsorption application. The consecutive adsorption–desorption cycle experiments were conducted: the Cot@β-CD fabric was firstly immersed into the MG dyes, and then washed with anhydrous ethanol and an appropriate 0.5 mol/L HCl (v/v = 4:3) in each cycle. Compared with the Pri-Cot, the Cot@β-CD fabric maintains good adsorption performance for dyes after five cycles (Fig. 5). Initially, the removal efficiency of MG on Cot@β-CD and Pri-Cot were respectively reached 93% and 65%, demonstrating that the modification of β-CD can effectively increase the adsorption capacity. After five adsorption–desorption cycles, due to the physically adsorbed β-CD loss from the fabric during the repeated elution, the removal efficiency of Cot@β-CD slightly decreased to 65%, but the removal efficiency of Pri-Cot decreased to only 30%.

TLC separation and SERS identification

Optimization of mobile phase

The high hydrophilicity and high porosity of cotton fiber can provide a porous network architecture, which contributes to the high fluid flow driven by capillary force in cotton fiber. The mobile phase solvent penetrates the TLC fabric, and transports the sample along the cotton fiber. The different interactions between the compounds, solvent system and TLC fabric cause the compounds to separate into individual components. The β-CD bonded stationary phase is suitable for multiple separation modes, and the appropriate mobile phase could be selected according to the structure and physical and chemical properties of the dyes. Therefore, the TLC tests were firstly performed on an optimization of mobile phase. The reference solutions of each dye were dropped on the white Cot@β-CD fabric. After development, spots in the chromatogram were visualized by the absorbance property. The development was evaluated from 0.5 mL of each dye (with a concentration of 10^{-3} M) with three kinds of mobile phase solvent: 1) cyclohexane: ethyl acetate (4:1, v/v), 2) dichloromethane: methanol (3:1, v/v) and 3) n-butanol: ethanol: 1% ammonia (3:1:1, v/v/v). The TLC images were shown in Fig. 6 (a: MG, b: RhB, c: CR and d: SD). Due to the different interactions between the dye molecules, solvent system and TLC fabrics, the development performance with solvents of different polarities showed an obvious difference. For the low polarity solvent 1, the MG, RhB and CR molecules were caught by the fabric and hardly ran with the solvents, while the SD ran fast with the solvent and approached to the solvent front accompanied by seriously diffusion. In the case of high polarity solvent 3, the RhB and SD molecules were transported along the solvent accompanied by obvious whole-journey tailing, while the MG and SD molecules showed slight movement. It was also observed that most of MG molecules fell off the cotton fabric into the solvent. In the case of solvent 2 with medium polarity, it was observed that CR would not move much, while three other dyes transported with the solvent at different distances depending on their different interaction. There is an obvious competition for different dye molecules by the Cot@β-CD (the stationary phase) and the solvent system (the mobile phase). Therefore, the solvent mixture of dichloromethane: methanol was selected as developing solvent to investigate two sets of mixed dyes (MG/SD and RhB/SD).

Changes in the volume ratio of the mixed solvents in the mobile phase may significantly affect the retention and resolution of the substance to be tested. In order to achieve the best resolution, the volume ratio of mixture solvent to perform better TLC separation was evaluated. It was found that increasing the volume fraction of dichloromethane, the two dyes are not completely separated, while increasing the volume fraction of methanol, the separated spots spread seriously. When regulating the volume ratio of dichloromethane and methanol as 3:1, the mixed dyes can be completely separated with good resolution (Fig. 7). As viewing by the adsorption and fluorescence properties, an R_f value of 0.85 for MG, and 0.83 for RhB and 0.78 for SD was obtained. These relatively high R_f values point out the stronger interactions between the analytes and the optimized mobile phase.

Recyclable separation performance of β-CD modified fabrics

Furthermore, the TLC separation performance of β-CD modified fabrics were demonstrated. It was observed that compared with the Pri-Cot (Fig. 8a), the Cot@β-CD fabric still showed better TLC separation with good resolution, though the sample spots spread a little (Fig. 8b). In addition, due to the excellent chemical stability of gold nanoparticles, the Cot@Au NPs@β-CD also could be used as TLC-SERS matrix for at least three times (Fig. 8c).

Integrated TLC separation and SERS identification of mixed dyes

After the separation on TLC based on the chemicals' different affinity with the stationary and mobile phase, compound chemical information with their characteristic Raman bands can be furtherly distinguished by SERS identification on the fabric-based TLC-SERS matrix. The above results demonstrated that the modified fabric performed excellent development and separation, the next step was to use the integrated gold nanoparticles as the SERS active substrate for dyes identification. 0.5 mL of the mixture solution of MG/SD or RhB/SD was pipetted onto the Cot@Au NPs@β-CD fabrics, and the chromatogram was developed using 3/1 (v/v) dichloromethane/methanol as the mobile phase. As shown in the optical photograph in Fig. 9A, before separation, the spots showed the color of the mixed solution of MG and SD, and after separation, the two separated spots were visualized by their own color, which can be marked visibly by the absorbance/fluorescence properties or according to their different R_f values if the deep-purple color of Cot@Au NPs@β-CD fabrics disturbed the visibly observation. After the evaporation of the solvent on the TLC fabrics, the fabrics were immediately scanned with Raman spectrometer to obtain their enhanced characteristic fingerprints. Excellent results were obtained by SERS, which provided remarkable signal enhancements and fluorescence suppression. The Raman spectrum of Cot@Au NPs@β-CD matrix was shown in curve 1, in which the band at 1120 cm^{-1} was attributed to the symmetric stretching vibration of the cellulose COC glycosidic bond and the COC ring breathing vibration, while the band at 1095 cm^{-1} was attributed to the asymmetric stretching vibration of the cellulose COC glycosidic bond. Curve 2–4 descripted the spectra of mixture dyes and two separated spots on the modified fabrics. Except for the bands of 1095 cm^{-1} belongs to the cotton fabric, a series of Raman bands at 1132 cm^{-1}, 1171 cm^{-1}, 1218 cm^{-1}, 1231 cm^{1}, 1389 cm^{-1}, 1441 cm^{-1}, 1467 cm^{-1}, 1594 cm^{-1} and

1615 cm^{-1} appeared in curve 2, some of which at 1132 cm^{-1}, 1231 cm^{-1}, 1441 cm^{-1}, 1467 cm^{-1} and 1594 cm^{-1} were found in curve 3 collected at spot 3 after separation, while some other bands at 1171 cm^{-1}, 1218 cm^{-1}, 1389 cm^{-1} and 1615 cm^{-1} were consistent with the Raman signals collected at spot 4 after separation. According to the fingerprint characteristics of the Raman spectrum reported previously (Hu et al. 2020; Ou et al. 2016), it can be proved that the spots 3 and 4 were respectively corresponds to the separated SD and MG, which is consistent with the result of absorbance visualization. The TLC separation and SERS identification of RhB/SD mixture were also conducted, as shown in Fig. 9B, it was found that with SERS spectrum of the dyes mixture not matching with the single SERS spectrum of the corresponding substances in mixtures. Interestingly, after TLC separation, the two SERS spectra were different from each other and they matched well with the SERS spectrum of separated component (RhB and SD), suggesting that RhB and SD could also be specifically identified *via* the TLC-SERS technique. Therefore, a novel use of TLC with on-site detection by SERS to generate chromatographic and spectral fingerprints of complex samples was realized. It demonstrated the feasibility and desirability for both the emergency and routine monitoring towards the dyes samples in art objects, textile and packaging products, as well as in trace evidence of forensic processes.

Conclusions

Cotton fabrics were functionalized by Au NPs *in situ* synthesized through a heating method. Porous β-CD was then covalently grafted onto Cot@Au NPs *via* esterification reaction. The multiple modification of fabric was endowed with the following functions: 1) dye separation, 2) preliminary TLC screening along with on-site SERS identification and 3) sustainable recyclable performance. A novel use of TLC with on-site detection by SERS to generate chromatographic and spectral fingerprints of complex samples (MG/SD and RhB/SD) was realized. Compared with the previous TLC-SERS method in which the SERS-active nanoparticles were added after development, constructing of stationary phase matrix and noble metallic active nanoparticles on the same fabric substrate greatly facilitates the fabrication and performance as well as eliminating interference from the migration of nanoparticles and analytes. Our future efforts will explore the full SERS mapping scan in a line or a large area on TLC fabrics to enhance the method sensitivity and precision, and then extend this study towards qualitative or quantitative of actual dye chemicals (such as artworks or lipsticks) with the help of chemometric tools for data analysis.

Declarations

CRediT authorship contribution statement

Huifang Yao: Data curation, Methodology, Writing - original draft.**Xiaxiao Dong**: Methodology, Formal analysis, Investigation, Writing - original draft.**Hong Xiong**: Formal analysis, Investigation. **Ji Zhou:**Conceptualization, Data curation, Methodology, Validation, Investigation, Writing - review & editing. **Yong Ye:** Investigation, Supervision, Writing - review & editing. ‡ These authors contributed equally.

competing interest

The authors declare that they have no known competing financial interests or personal relationships that could have appeared to influence the work reported in this paper.

Acknowledgments

This research was supported by the Fund of Science and Technology on Surface Physics and Chemistry Laboratory (6142A02190104), Key Project of the Institute of Forensic Technology Application and Social Governanceof Zhongnan University of Economics and Law (FSSGL2021B-03).

References

1. Abdel-Halim ES, Al-Deyab SS, Alfaifi AY (2014) Cotton fabric finished with beta-cyclodextrin: Inclusion ability toward antimicrobial agent. Carbohyd Polym 102:550-556.https://doi:10.1016/j.carbpol.2013.11.074
2. Alzate-Sánchez DM, Smith BJ, Alsbaiee A, Hinestroza JP, Dichtel WR (2016) Cotton fabric functionalized with a β-Cyclodextrin polymer captures organic pollutants from contaminated air and water.Chem Mater 28:8340-8346.https://doi:10.1021/acs.chemmater.6b03624
3. Bao W, Zhang C, Yang M, Nan D, Liu T, Guo X, Fang L (2021) Preparation and modeling study of novel carboxymethyl-β-cyclodextrin silica hybrid monolithic column for enantioseparations in capillary electrochromatography. Microchem J 170:106719. https://doi.org/10.1016/j.microc.2021.106719
4. Boscacci M, Francone S, Galli K, Bruni S (2020) The brightest colors: A Fourier-transform Raman, surface-enhanced Raman, and thin-layer chromatography-surface-enhanced Raman spectroscopy study of fluorescent artists' paints. JRaman Spectrosc 51:1108-1117.https://doi:10.1002/jrs.5868
5. Cañamares MV, Reagan DA, Lombardi JR, Leona M (2014) TLC-SERS of mauve, the first synthetic dye.J Raman Spectrosc 45:1147-1152. https: //doi.org/10.1002/jrs.4508
6. Cesaratto A, Leona M, Pozzi F (2019) Recent advances on the analysis of polychrome works of art: SERS of synthetic colorants and their mixtures with natural dyes. Front Chem 7:105.https://doi.org/10.3389/fchem.2019.00105
7. Fang F, Qi Y, Lu F, Yang L (2016) Highly sensitive on-site detection of drugs adulterated in botanical dietary supplements using thin layer chromatography combined with dynamic surface enhanced Raman spectroscopy. Talanta 146:351-357.https://doi.org/10.1016/j.talanta.2015.08.067
8. Freye CE, Crane NA, Kirchner TB, Sepaniak MJ (2013) Surface enhanced Raman scattering imaging of developed thin-layer chromatography plates. Anal Chem 85:3991-3998.https://doi.org/10.1021/ac303710q
9. Gu X, Jin Y, Dong F, Cai Y, You Z, You J, Zhang L, Du S (2018) Toward rapid analysis, forecast and discovery of bioactive compounds from herbs by jointly using thin layer chromatography and ratiometric surface-enhanced Raman spectroscopy technique. J Pharmaceut Biomed 153:9-15.https://doi.org/10.1016/j.jpba.2018.02.016

10. Hu B, Sun DW, Pu H, Wei Q (2020) A dynamically optical and highly stable pNIPAM @ Au NRs nanohybrid substrate for sensitive SERS detection of malachite green in fish fillet. Talanta 218:121188.https://doi.org/10.1016/j.talanta.2020.121188
11. Kim K-S, Choi S, Cha J-H, Yeon S-H, Lee H (2006) Facile one-pot synthesis of gold nanoparticles using alcohol ionic liquids. J Mater Chem 16:1315-1317.https://doi.org/10.1039/B601478J
12. Kong X, Squire K, Chong X, Wang AX (2017) Ultra-sensitive lab-on-a-chip detection of sudan I in food using plasmonics-enhanced diatomaceous thin film. Food Control 79:258-265.https://doi.org/10.1016/j.foodcont.2017.04.007
13. Li D, Qu L, Zhai W, Xue J, Fossey JS, Long Y (2011) Facile on-site detection of substituted aromatic pollutants in water using thin layer chromatography combined with surface-enhanced Raman spectroscopy. Environ Sci Technol 45:4046-4052.https://doi.org/10.1021/es104155r
14. Li H, Zhu Q, Chwee T, Wu L, Chai Y, Lu F, Yuan Y (2015) Detection of structurally similar adulterants in botanical dietary supplements by thin-layer chromatography and surface enhanced Raman spectroscopy combined with two-dimensional correlation spectroscopy. Anal Chim Acta 883:22-31.https://doi.org/10.1016/j.aca.2015.04.017
15. Li Y, Zhao C, Lu C, Zhou S, Tian G, He L, Bao Y, Fauconnier M-L, Xiao H, Zheng J (2021) Simultaneous determination of 14 bioactive citrus flavonoids using thin-layer chromatography combined with surface enhanced Raman spectroscopy. Food Chem 338:128115.https://doi.org/10.1016/j.foodchem.2020.128115
16. Ma J, Xu W, Kou X, Niu Y, Xia Y, Wang Y, Tian G, Zhao Y, Ke, Q (2020) Green fabrication of control-released, washable, and nonadhesives aromatic-nanocapsules/cotton fabrics via electrostatic-adsorption/in situ immobilization. ACS Sustainable Chem Eng 8:15258-15267.https://doi.org/10.1021/acssuschemeng.0c05040
17. Minh DTC, Thi LA, Huyen NTT, Van Vu L, Anh NTK, Ha PTT (2019) Detection of sildenafil adulterated in herbal products using thin layer chromatography combined with surface enhanced Raman spectroscopy: "Double coffee-ring effect" based enhancement.J Pharmaceut Biomed 174:340-347.https://doi.org/10.1016/j.jpba.2019.05.043
18. Ou Y, Pei L, Lai K, Huang Y, Rasco BA, Wang X, Fan Y (2016) Rapid analysis of multiple sudan dyes in chili flakes using surface-enhanced Raman spectroscopy coupled with Au–Ag core-shell nanospheres. Food Anal Method 10:565-574.https://doi.org/10.1007/s12161-016-0618-z
19. Patil NV, Netravali AN (2019) Cyclodextrin-based “green” wrinkle-free finishing of cotton fabrics. Ind Eng Chem Res 58:20496-20504.https://doi.org/10.1021/acs.iecr.9b04092
20. Pereira JC, Marques JMC, Wlodarczyk E, Fenert B, Zarzycki PK (2018) Toward the understanding of micro-TLC behavior of various dyes on silica and cellulose stationary phases using adata mining approach. J AOAC Int 101:1437-1447.https://doi.org/10.5740/jaoacint.18-0061
21. Pilot R (2018) SERS detection of food contaminants by means of portable Raman instruments.J Raman Spectrosc 49:954-981.https://doi.org/10.1002/jrs.5400

22. Popescu V, Petrea M, Popescu A (2021) Multifunctional finishing of cotton with compounds derived from MCT-beta-CD and quantification of effects using MLR statistical analysis. Polymers 13:410.https://doi.org/10.3390/polym13030410
23. Pozzi F, Shibayama N, Leona M, Lombardi JR (2013) TLC-SERS study of Syrian rue (Peganum harmala) and its main alkaloid constituents.J Raman Spectrosc 44:102-107.https://doi.org/10.1002/jrs.4140
24. Qu LL, Jia Q, Liu C, Wang W, Duan L, Yang G, Han C-Q, Li H (2018) Thin layer chromatography combined with surface-enhanced raman spectroscopy for rapid sensing aflatoxins. J Chromatogr A 1579:115-120.https://doi.org/10.1016/j.chroma.2018.10.024
25. Rojanarata T, Plianwong S, Su-uta K, Opanasopit P, Ngawhirunpat T (2013) Electrospun cellulose acetate nanofibers as thin layer chromatographic media for eco-friendly screening of steroids adulterated in traditional medicine and nutraceutical products. Talanta 115:208-213.https://doi.org/10.1016/j.talanta.2013.04.078
26. Schenk C, Kutzscher C, Drache F, Helten S, Senkovska I, Kaskel S (2017) Metal-organic frameworks for thin-layer chromatographic applications. ACS Appl Mater Inter 9:2006-2009.https://doi.org/10.1021/acsami.6b13092
27. Sciutto G, Prati S, Bonacini I, Litti L, Meneghetti M, Mazzeo R (2017) A new integrated TLC/MU-ATR/SERS advanced approach for the identification of trace amounts of dyes in mixtures. Anal Chim Acta 991:104-112.https://doi.org/10.1016/j.aca.2017.08.020
28. Shen Z, Fan Q, Yu Q, Wang R, Wang H, Kong X (2021a) Facile detection of carbendazim in food using TLC-SERS on diatomite thin layer chromatography. Spectrochim Acta Part A Mol Biomol Spectrosc 247:119037.https://doi.org/10.1016/j.saa.2020.119037
29. Shen Z, Wang H, Yu Q, Li Q, Lu X, Kong X (2021b) On-site separation and identification of polycyclic aromatic hydrocarbons from edible oil by TLC-SERS on diatomite photonic biosilica plate. Microchem J 160:105672.https://doi.org/10.1016/j.microc.2020.105672
30. Soares FLF, Ardila JA, Carneiro RL (2017) Thin-layer chromatography-surface-enhanced Raman spectroscopy and chemometric tools applied to Pilsner beer fingerprint analysis. J Raman Spectrosc 48:943-950.https://doi.org/10.1002/jrs.5168
31. French AD, Cintrón MS (2013) Cellulose polymorphy, crystallite size, and the SegalCrystallinity Index. Cellulose 20:583-588. https://doi.org/10.1007/s10570-012-9833-y
32. French AD (2014) Idealized powder diffraction patterns for cellulosepolymorphs. Cellulose 21:885-896. https://doi.org/10.1007/s10570-013-0030-4
33. Tan A, Zhao Y, Sivashanmugan K, Squire K, Wang AX (2019) Quantitative TLC-SERS detection of histamine in seafood with support vector machine analysis. Food Control 103:111-118.https://doi.org/10.1016/j.foodcont.2019.03.032
34. Tang B, Lin X, Zou F, Fan Y, Li D, Zhou J, Chen W, Wang X (2017) In situ synthesis of gold nanoparticles on cotton fabric for multifunctional applications. Cellulose 24:4547-4560.https://doi.org/10.1007/s10570-017-1413-8

35. Tang B, Zhang M, Hou X, Li J, Sun L, Wang X (2012) Coloration of cotton fibers with anisotropic silver nanoparticles. IndEng Chem Res 51:12807-12813.https://doi.org/10.1021/ie3015704
36. Tang RH, Liu LN, Zhang SF, He XC, Li XJ, Xu F, Ni YH, Li F (2019) A review on advances in methods for modification of paper supports for use in point-of-care testing. Mikrochim Acta 186:521.https://doi.org/10.1007/s00604-019-3626-z
37. Wang Y, Wang X, Sun Q, Li R, Ji Y (2021) Facile separation of enantiomers via covalent organic framework bonded stationary phase. Mikrochim Acta 188:367.https://doi.org/10.1007/s00604-021-04925-8
38. Weatherston JD, Yuan S, Mashuga CV, Wu HJ (2019) Multi-functional SERS substrate: collection, separation, and identification of airborne chemical powders on a single device. Sensor Actuat B-Chem 297:126765.https://doi.org/10.1016/j.snb.2019.126765
39. Woodhead AL, Cosgrove B, Church JS (2016) The purple coloration of four late 19th century silk dresses: A spectroscopic investigation.Spectrochim Acta Part A Mol Biomol Spectrosc 154:185-192.https://doi.org/10.1016/j.saa.2015.10.024
40. Wu Q, Gao J, Chen L, Dong S, Li H, Qiu H, Zhao L (2019) Graphene quantum dots functionalized beta-cyclodextrin and cellulose chiral stationary phases with enhanced enantioseparation performance.J Chromatogr A 1600:209-218.https://doi.org/10.1016/j.chroma.2019.04.053
41. Xiao Y, Ng SC, Tan TT, Wang Y (2012) Recent development of cyclodextrin chiral stationary phases and their applications in chromatography.J Chromatogr A 1269:52-68.https://doi.org/10.1016/j.chroma.2012.08.049
42. Zhang BB, Shi Y, Chen H, Zhu QX, Lu F, Li YW (2018) A separable surface-enhanced Raman scattering substrate modified with MIL-101 for detection of overlapping and invisible compounds after thin-layer chromatography development. Anal Chim Acta 997:35-43.https://doi.org/10.1016/j.aca.2017.10.006
43. Zhang ZM, Liu JF, Liu R, Sun JF, Wei GH (2014) Thin layer chromatography coupled with surface-enhanced Raman scattering as a facile method for on-site quantitative monitoring of chemical reactions. Anal Chem 86:7286-7292.https://doi.org/10.1021/ac5017387
44. Zhao Y, Tan A, Squire K, Sivashanmugan K, Wang AX (2019) Quaternion-based parallel feature extraction: extending the horizon of quantitative analysis using TLC-SERS Sensing.Sensor Actuat B-Chem 299:126902.https://doi.org/10.1016/j.snb.2019.126902
45. Zhu Q, Cao Y, Li D, Fang F, Lu F, Yuan Y (2019) A fast response TLC-SERS substrate for on-site detection of hydrophilic and hydrophobic adulterants in botanical dietary supplements. New J Chem 43:13873-13880.https://doi.org/10.1039/c9nj02489a
46. Zhu Q, Li H, Lu F, Chai Y, Yuan Y (2016) A widely applicable silver sol for TLC detection with rich and stable SERS features. Nanoscale Res Lett 11:220.https://doi.org/10.1186/s11671-016-1442-5

Figures

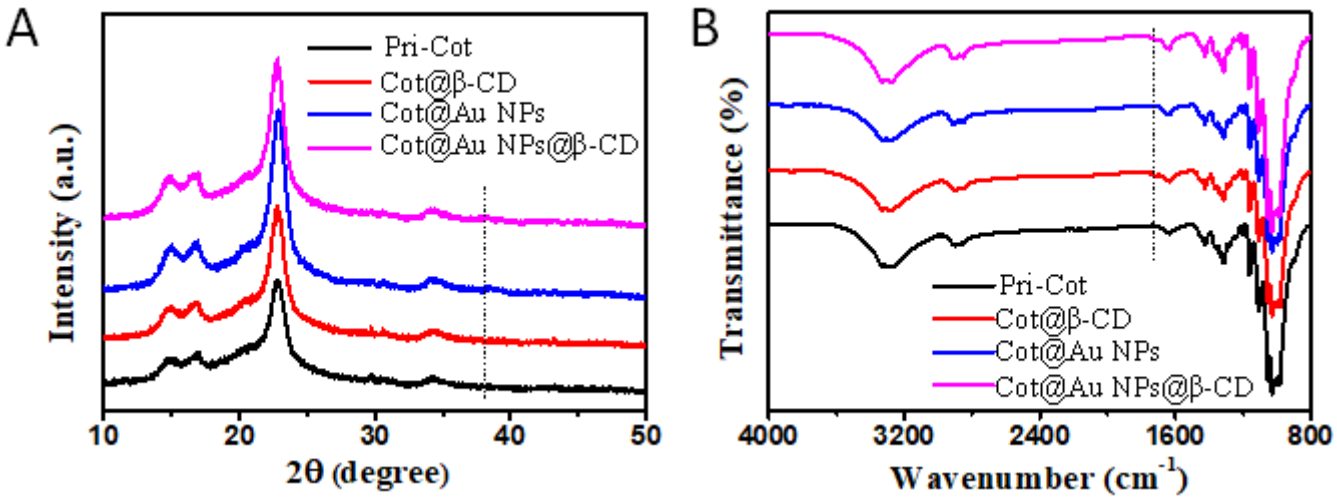

Figure 1

XRD curves (A) and FTIR spectra (B) of Pri-Cot, Cot@β-CD, Cot@Au NPs and Cot@Au NPs@β-CD

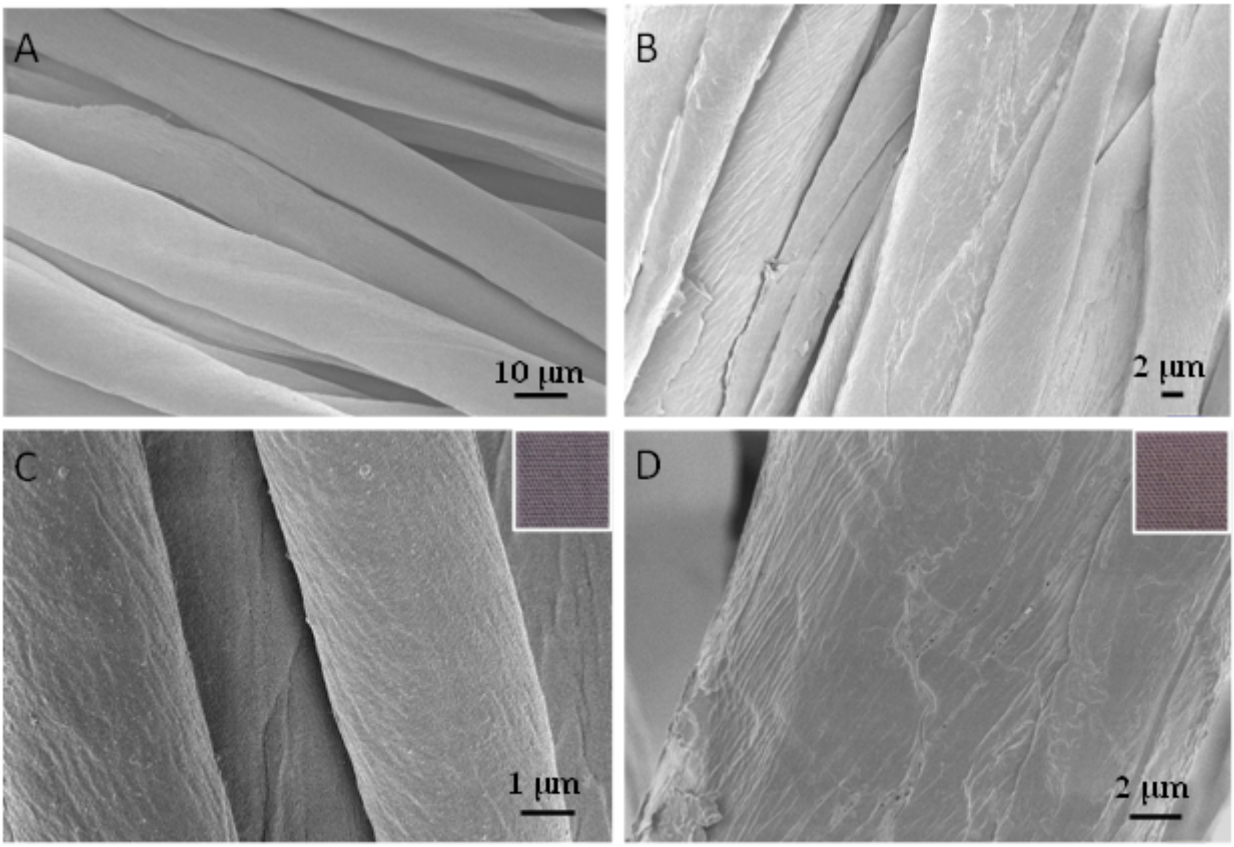

Figure 2

SEM images of (A) Pri-Cot, (B) Cot@β-CD, (C) Cot@Au NPs, (D) Cot@Au NPs@β-CD (Inset: photograph of the (C) Cot@Au NPs, (D) Cot@Au NPs@β-CD exhibiting deep-purplecolor)

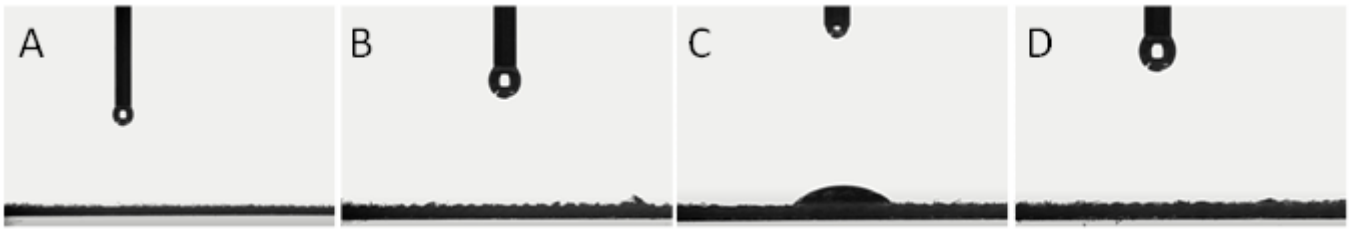

Figure 3

Wettability of treated cotton fabris: (A) Pri-Cot, (B) Cot@β-CD, (C) Cot@Au NPs, and (D) Cot@Au NPs@β-CD

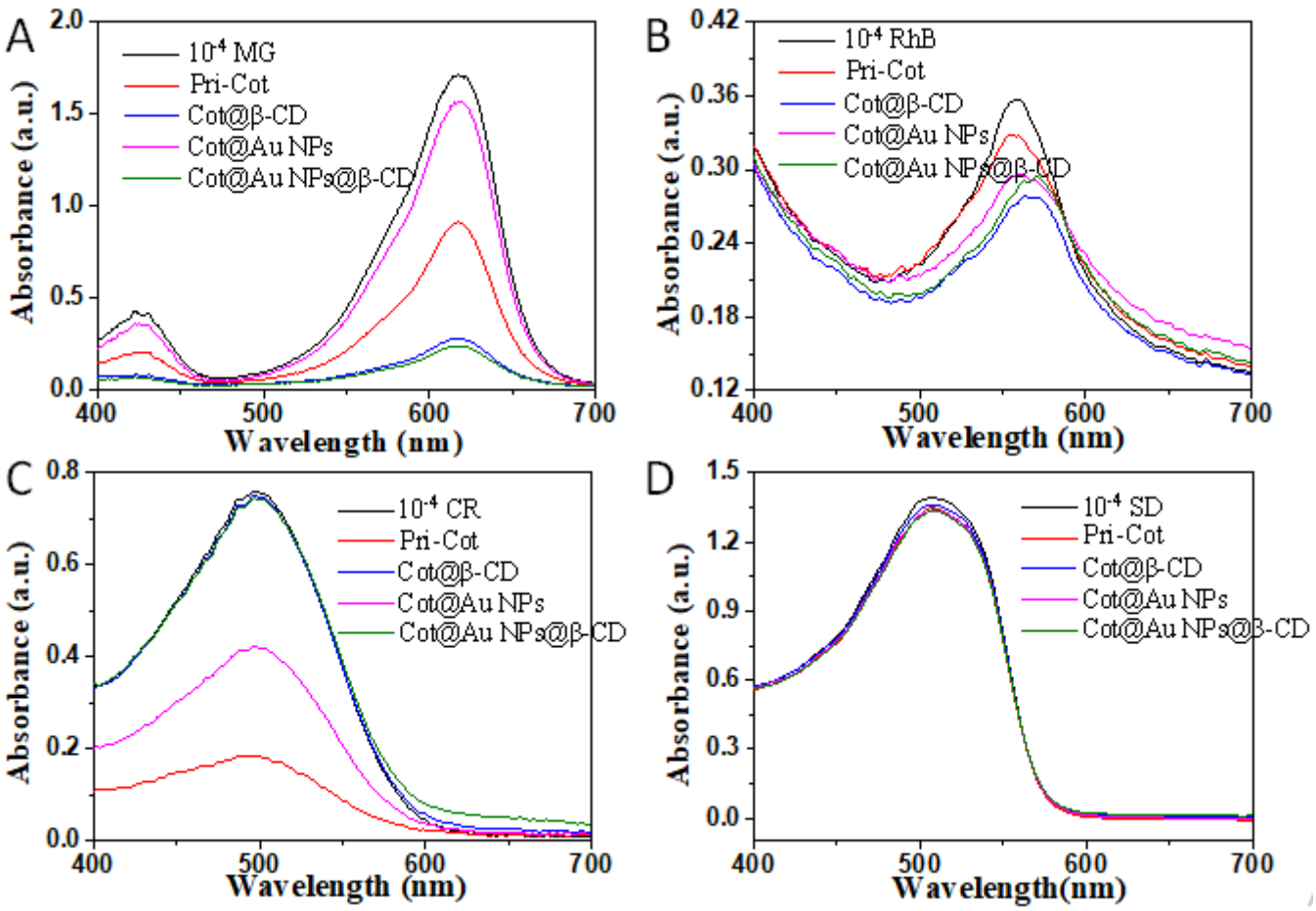

Figure 4

UV–vis absorption of initial and the residue dye solution of (A) MG, (B) RhB, (C) CR and (D) SDafter incubated withPri-Cot,Cot@β-CD,Cot@Au NPs and Cot@Au NPs@β-CD

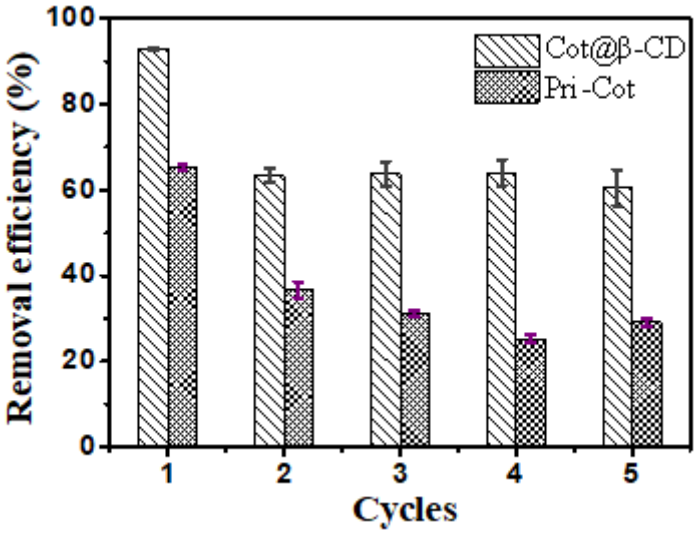

Figure 5

Removal efficiencyof MG adsorbed onto the Cot@β-CD and Pri-Cotwithin five adsorption–desorption cycle experiments

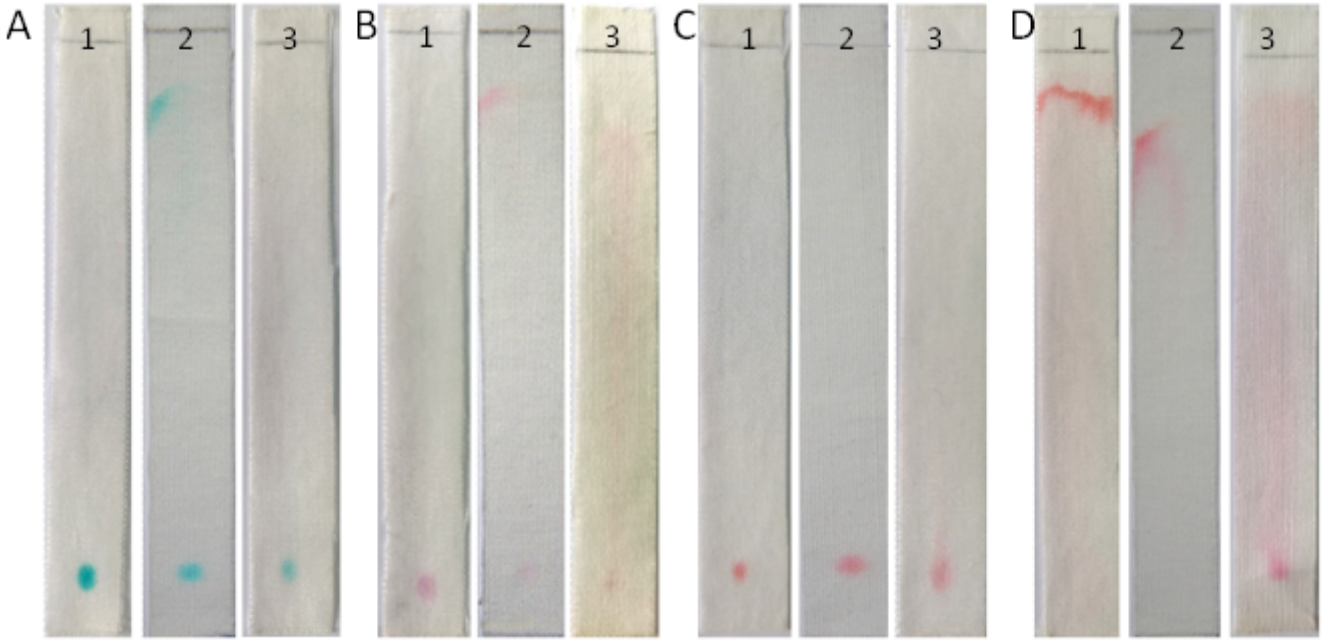

Figure 6

TLC imagesof four reference dyes on the Cot@β-CD fabrics, (A) MG, (B) RhB, (C) CR and (D) SD with solvent 1-cyclohexane: ethyl acetate (4:1, v/v), 2-dichloromethane: methanol (3:1, v/v) and 3-n-butanol: ethanol: 1% ammonia (3:1:1, v/v/v), respectively

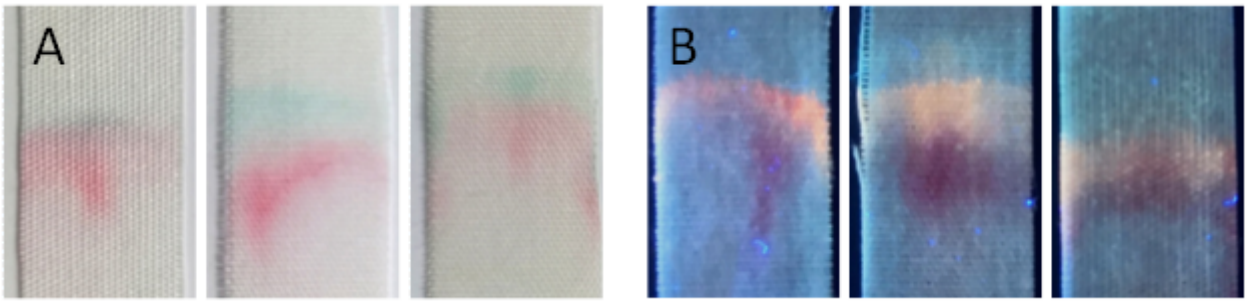

Figure 7

TLC separation of the mixed dyes of A)MG/SD (visible by the adsorption), B)RhB/SD (visible by the fluorescence) on Cot@β-CD fabrics by using dichloromethane and methanol as mobile phase. The volume ratio from left to right are 7:2, 3:1, 3:2, respectively

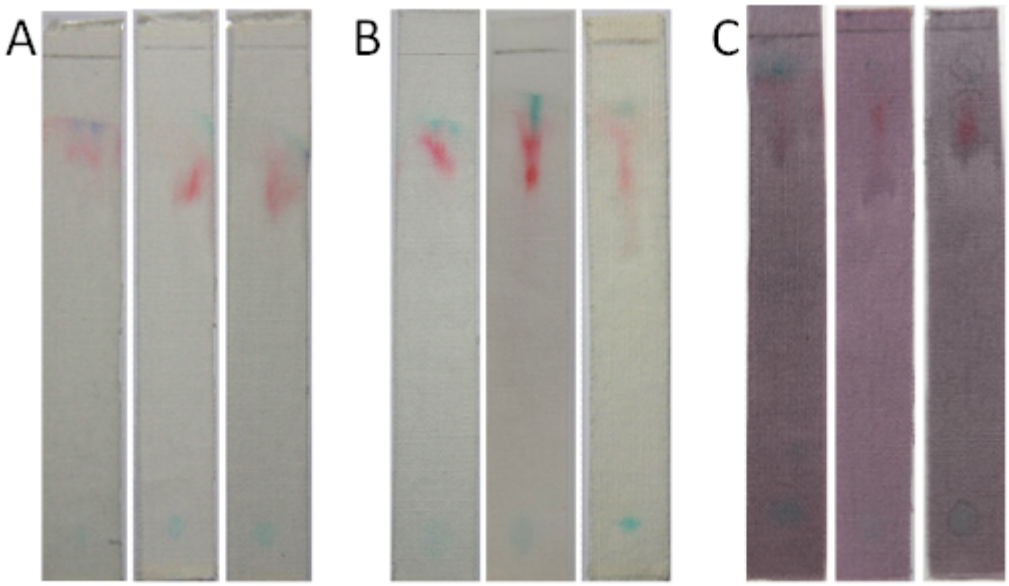

Figure 8

TLC results of the analysis of MG/SD on (A) Pri-Cot, (B)Cot@β-CD,and (C)Cot@Au NPs@β-CDafter three cycle experiments

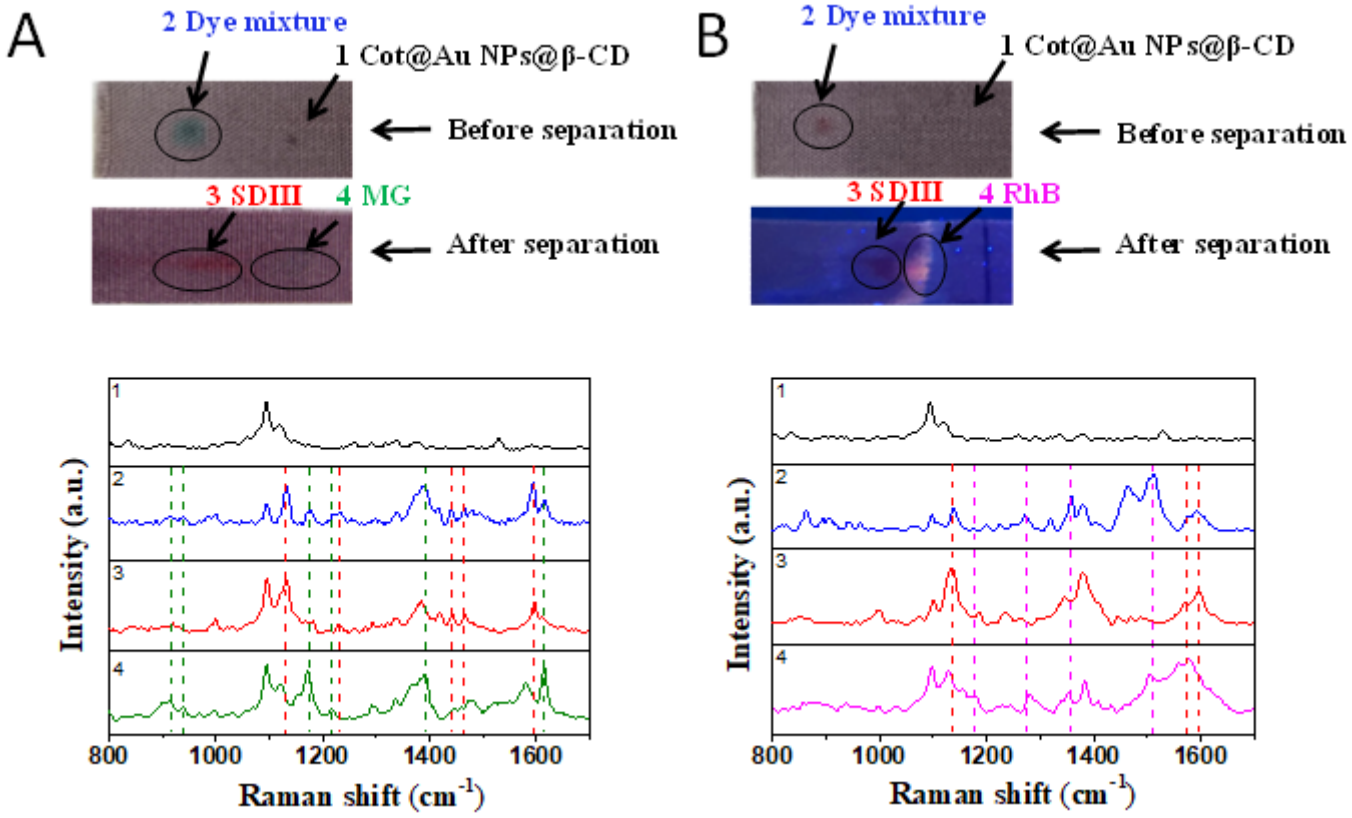

Figure 9

The optical images of the Cot@Au NPs@β-CD fabrics before and after separation, and SERS spectra obtained from the spot 1 of the Cot@Au NPs@β-CD fabrics, the spot 2 of sample mixture without TLC separation, and spots 3 and 4 on the TLC plate after separation (A) MG/SD and (B) RhB/SD

Supplementary Files

This is a list of supplementary files associated with this preprint. Click to download.

- Scheme1.png